Research Article

Catalytic Activity of ZrO$_2$ Nanotube Arrays Prepared by Anodization Method

Xixin Wang, Jianling Zhao, Xiaorui Hou, Qi He, and Chengchun Tang

School of Material Science and Engineering, Hebei University of Technology, Tianjin 300130, China

Correspondence should be addressed to Jianling Zhao, zhaojl02@mails.tsinghua.edu.cn

ZrO$_2$ nanotube arrays were prepared by anodization method in aqueous electrolyte containing $(NH_4)_2SO_4$ and NH_4F. The morphology and structure of nanotube arrays were characterized through scanning electron microscope, X-ray diffraction, and infrared spectra analysis. The zirconia nanotube arrays were used as catalyst in esterification reaction. The effects of calcination temperature and electrolyte concentration on catalytic esterification activity have been investigated in detail. Experiments indicate that nanotube arrays have highest catalytic activity when the concentration of $(NH_4)_2SO_4$ is 1 mol/L, the concentration of NH_4F is 1 wt%, and the calcination temperature is 400°C. Esterification reaction yield of as much as 97% could be obtained under optimal conditions.

1. Introduction

ZrO$_2$, due to its excellent physical and chemical properties, is widely used in catalysis field. For example, it can be used as catalyst or catalyst carrier in Fischer-Tropsch synthesis, polymerization, isomerization, alkylation and esterification reaction, and so forth [1–4]. In addition, it can also be used in environment and energy aspects including synthesis of biodiesel and catalytic purification of harmful gas [5–9].

The structure and morphology of ZrO$_2$ have significant effect on its catalytic activity. ZrO$_2$ nanoparticles can improve catalytic activity due to their large specific surface area [10–12]. However, nanoparticles are difficult to be separated from the reaction medium, and loss quantity is large during the recycle process. Thus, the improvement of ZrO$_2$ nanocatalysts needs further exploration.

ZrO$_2$ nanotube arrays have been prepared by anodization method in recent years [13–16]. The nanotube arrays with large specific surface area and tubular structure can be used as nanoreactors. In addition, nanotube arrays are easy to be removed from the reaction system due to their big size. Therefore, ZrO$_2$ nanotube arrays may have a wide application prospect in the field of catalyst. However, few studies have been done on the application of ZrO$_2$ nanotube arrays

in catalysis field. In this paper, ZrO$_2$ nanotube arrays prepared by anodization method in the electrolyte containing SO_4^{2-} are directly used as catalyst in the esterification reaction. The effects of calcination temperature and electrolyte concentration on catalytic esterification activity have been investigated in detail.

2. Experimental

2.1. Preparation of Zirconia Nanotube Arrays Catalyst. Zirconia nanotube arrays were prepared by anodization method in aqueous electrolyte containing 1 M $(NH_4)_2SO_4$ and 1 wt% NH_4F. Zirconium foil was pretreated according to the method given [17]. Zirconium foil was anode and platinum electrode was cathode, and the distance between two electrodes was 2 cm. The initial voltage was 3 V, and then the voltage was increased at the rate of 3 V/30 min. At the beginning of anodization, a film of dense oxides would fabricate at the surface of zirconium foil which has retarding effect on the oxidation reaction. Increasing the voltages step by step would decrease thickness of the film and enhance the reaction's uniformity. After anodization for 2.5 h, nanotube arrays were peeled off from zirconium foil, dried at 100°C, and calcined for 60 min to obtain the zirconia nanotube arrays catalyst.
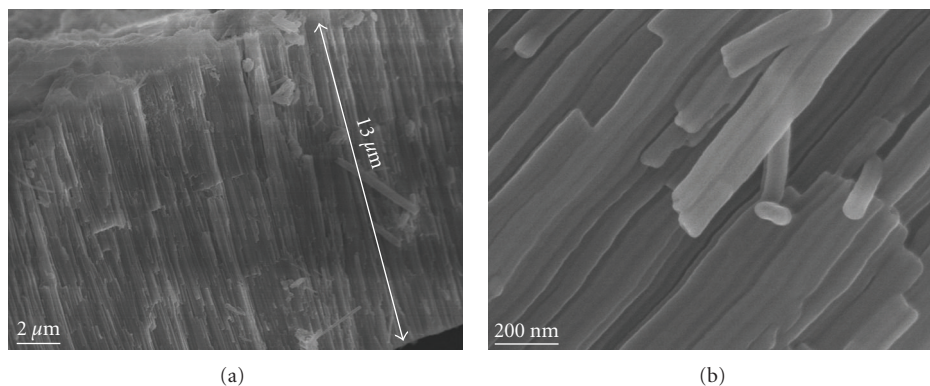
(a)

(b)

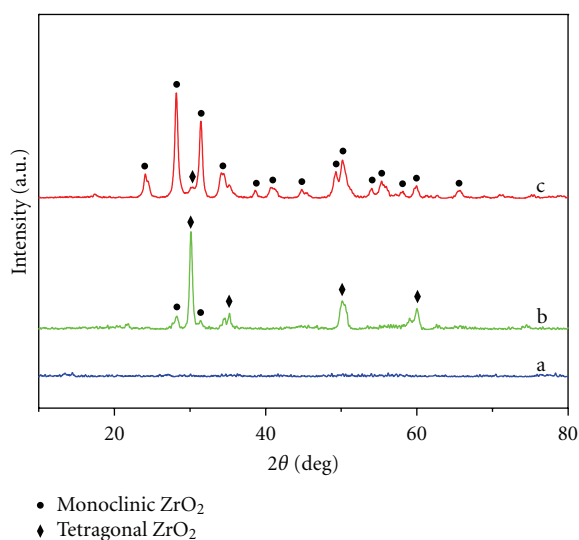FIGURE 1: The morphology of zirconia nanotube arrays.

- • Monoclinic ZrO_2
- ♦ Tetragonal ZrO_2

FIGURE 2: The XRD patterns of zirconia nanotube arrays calcined at: (a) 200°C, (b) 400°C, (c) 600°C.

FIGURE 3: Influences of calcination temperatures on catalytic activity.

2.2. Characterization of the Catalyst.

The morphologies of nanotube samples were observed through Philips XL 30 TMP scanning electron microscope (SEM, 20 kV accelerating voltage). Crystal phase analysis of the samples was conducted through Philips X' pert MPD X-ray powder diffraction analyzer (XRD, copper target, 50 kV, 40 mA, the length of scanning step was 0.04°, and the scope of scanning was 10°– 80° (2θ)). The samples calcined at different temperatures were characterized by Fourier transform infrared spectrometer (FTIR, WQF-410, China) with a scanning scope of 400~4000 cm^{-1}.

2.3. Catalytic Activity Experiment.

Esterification reactions were carried out in a reflux system. Absolute alcohol and propionic acid (mole ratio = 2 : 1) were added into a three-neck flask. The catalyst accounting for 2 wt% of the total amount of reaction solution was added. The reaction solution was refluxed at 85°C for 60 min. After the reacti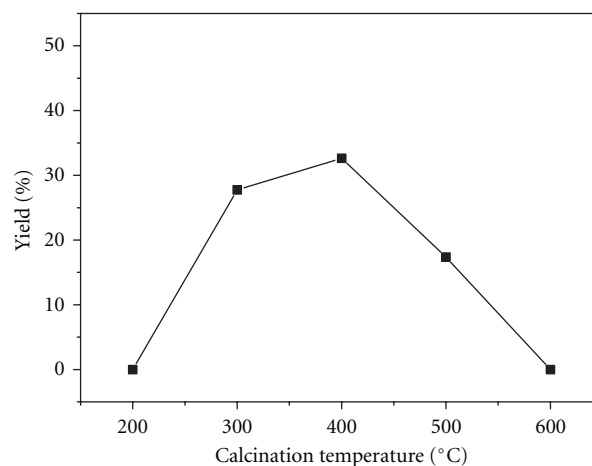on, the product was cooled, and the esterification yield was determined through gas chromatography analysis (GC1100, P-general, China).

3. Results and Discussion

Figure 1 shows the morphology of zirconia nanotube arrays prepared by anodizing zirconium foil in aqueous electrolyte containing 1 M $(NH_4)_2SO_4$ and 1 wt% NH_4F for 2.5 h. As shown in Figure 1, average diameter of the nanotube is up to 70 nm, and the average length is up to 13 μm. The nanotubes' structure has no obvious changes when the annealed temperature is lower than 600°C, and it would be destroyed to some extent at higher temperatures [18].

Figure 2 shows the XRD patterns of zirconia nanotube arrays calcined at different temperatures. The nanotube samples are amorphous at 200°C (Figure 2(a)). Two mixed crystal structures of tetragonal phase (accounting for 84%, pdf Card no. 80-784) and monoclinic phase (accounting for 16%) emerged at 400°C (Figure 2(b)). When calcined at 600°C, the nanotube samples are mainly composed of monoclinic phase (accounting for 90%, pdf Card no. 37-1484) and a little tetragonal phase (accounting for 10%, Figure 2(c)).
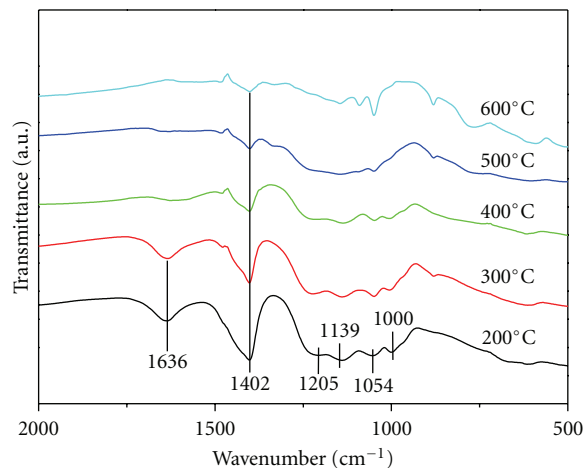
FIGURE 4: Infrared spectra of zirconia nanotube arrays catalyst calcined at different temperatures.

As is calculated from Scherrer formula, the average grain size is 18–26 nm after calcined.

Zirconia nanotube arrays calcined at different temperatures were used as catalyst, and the esterification reactions were carried out under the same conditions as given in Section 2.3. Figure 3 shows the influence of calcination temperatures on the catalytic activity of zirconia nanotube arrays. The catalytic activity first increases and then decreases with the increase of calcination temperature, reaching the maximum value at 400°C.

The FTIR spectra of zirconia nanotube arrays calcined at different temperatures are shown in Figure 4. The infrared absorption band at $1636 \, cm^{-1}$ appeared below 400°C is assigned to NH_4^+. The reason might be that zirconia nanotube arrays were prepared in electrolyte containing $(NH_4)_2SO_4$ and NH_4F. During the preparation process, quite a number of NH_4^+ were adsorbed by the sample. Ammonium salt would decompose gradually with the increase of temperature. It would decompose completely, and the infrared absorption band at $1636 \, cm^{-1}$ disappeared when the temperature is higher than 400°C. The infrared absorption bands at $1205 \, cm^{-1}$, $1139 \, cm^{-1}$, $1054 \, cm^{-1}$ and $1000 \, cm^{-1}$, are assigned to chelate complex between sulfate ion and zirconium ion. The increase of calcination temperature would lead to the desorption of SO_4^{2-} and the decrease of adsorption strength [19].

The infrared absorption band at $1402 \, cm^{-1}$ is assigned to surface hydroxyl group and adsorbed water. Along with the increase of the temperature, adsorbed water would desorb, and part of surface hydroxyl group would cross-link and dehydrate and result in decrease of the absorption band intensity at $1402 \, cm^{-1}$.

According to the infrared spectra analysis, calcination temperature affects the catalytic activity through the formation of solid acid structure. Along with the increase of temperature, electrolyte adsorbed by the nanotubes would decompose, and ZrO_2 would react with SO_4^{2-} to form solid acid structure on the surface of nanotube arrays. Thus, the

catalyst activity can be improved obviously. When the calcination temperature is too high, the structure of solid acid would decompose, and the catalyst activity would decrease. In addition, XRD and IR analysis shows that different calcination temperatures would result in the different crystal structures and surface properties, which would influence the combination of SO_4^{2-} and zirconia and lead to the changes of catalytic activities.

Electrolyte concentration has a great influence on catalytic activity. Figure 5(a) shows the influence of the $(NH_4)_2SO_4$ concentration on the catalytic activity. With the increase of $(NH_4)_2SO_4$ concentration, the esterification yield increases gradually. When the concentration of $(NH_4)_2SO_4$ is over 1.0 M, the yield changes much slowly. The reason might be that the higher the concentration is, the more SO_4^{2-} is adsorbed by nanotubes, and the more active centers form at the catalyst. When the concentration is over 1.0 M, the SO_4^{2-} adsorbed by nanotubes is close to saturation. Therefore, further increase of the $(NH_4)_2SO_4$ concentration has no more distinct effect on the improvement of catalytic activity.

Figure 5(b) shows the influence of the NH_4F concentration on catalytic activity. With the increase of NH_4F concentration, the esterification yield increases first and then decreases. When the NH_4F concentration is 1.0 wt%, the yield is highest. The partial dissolution of nanotube arrays in electrolyte solution containing F^- results in rougher surface and bigger specific surface area. Thus, the catalytic activity increases accordingly. But excessive dissolution would destroy the structure of nanotube arrays and lead to the decrease of catalytic activity.

According to the results discussed above, zirconia nanotube arrays were prepared by anodization method in aqueous electrolyte containing 1 M $(NH_4)_2SO_4$ and 1 wt% NH_4F, followed by calcination at 400°C for 60 min. Taking the nanotubes as catalyst, esterification reaction between dodecanol and propionic acid was conducted at 130°C to produce dodecyl propanoate. The yield is 95.4% when reaction time is 120 min (Figure 6(a)). For the reaction between dodecanol
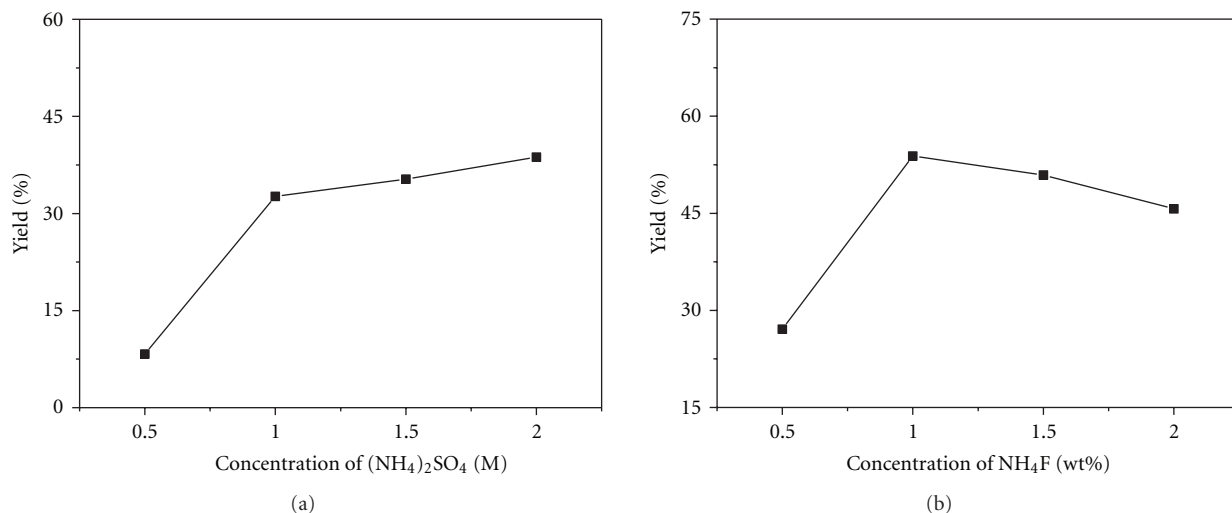
(a)

(b)

FIGURE 5: Influences of electrolyte concentration on catalytic activity: (a) $(NH_4)_2SO_4$, (b) NH_4F.
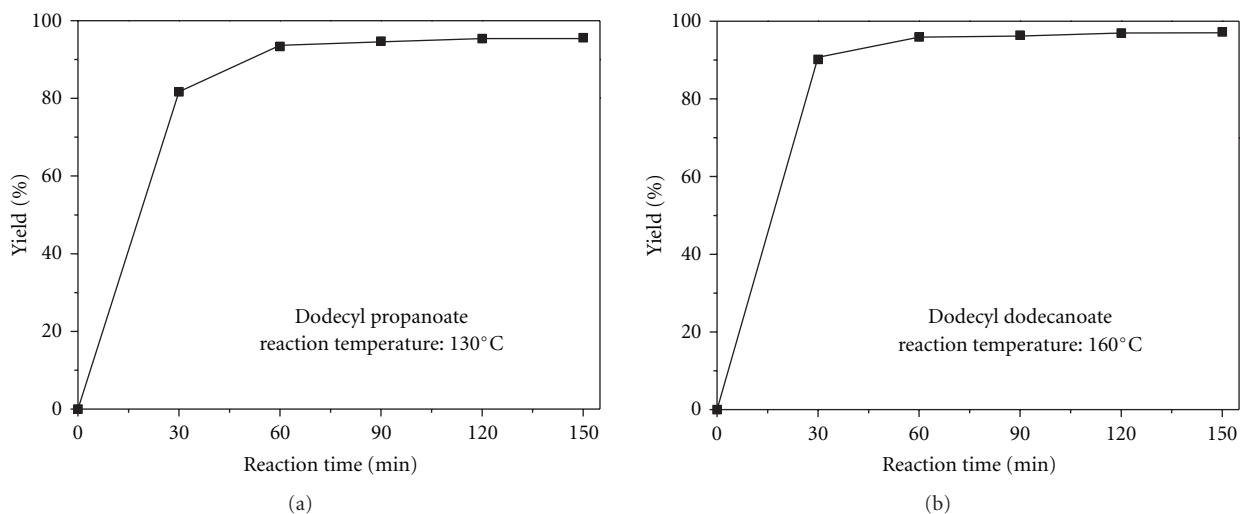

(a)

(b)

FIGURE 6: Catalytic activity of ZrO_2 nanotube arrays.

and lauric acid at 160°C, the yield of dodecyl laurate is 95.9 % when reaction time is 60 min. When reaction time was extended to 150 min, the yield is as high as 97.3% (Figure 6(b)).

4. Conclusion

ZrO_2 nanotube arrays were prepared by anodization method in aqueous electrolyte containing $(NH_4)_2SO_4$ and NH_4F. ZrO_2 nanotube arrays after calcination exhibit good catalytic activity in esterification reaction. Calcination temperature and electrolyte concentration have a great influence on catalytic activity. The ZrO_2 nanotube catalyst which was prepared in aqueous electrolyte containing 1 M $(NH_4)_2SO_4$ and 1 wt% NH_4F exhibits highest catalytic activity after calcined at 400°C. The yield of esterification reaction between

dodecanol and lauric acid could reach more than 97%, and the yield of esterification reaction between dodecanol and propionic acid could reach more than 95%.
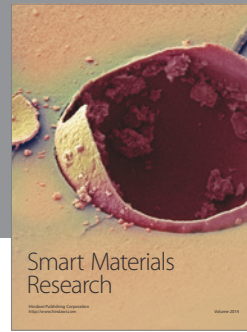
References

[1] N. Yamamoto, S. Sato, R. Takahashi, and K. Inui, "Synthesis of 3-buten-1-ol from 1,4-butanediol over ZrO_2 catalyst," *Journal of Molecular Catalysis A*, vol. 243, no. 1, pp. 52–59, 2006.

[2] A. I. Ahmed, S. A. El-Hakam, S. E. Samra, A. A. EL-Khouly, and A. S. Khder, "Structural characterization of sulfated zirconia and their catalytic activity in dehydration of ethanol," *Colloids and Surfaces A*, vol. 317, no. 1–3, pp. 62–70, 2008.

[3] M. H. Youn, J. G. Seo, S. Park et al., "Hydrogen production by auto-thermal reforming of ethanol over Ni-Ti-Zr metal oxide catalysts," *Renewable Energy*, vol. 34, no. 3, pp. 731–735, 2009.

[4] S. Chokkaram and B. H. Davis, "Dehydration of 2-octanol over zirconia catalysts: influence of crystal structure, sulfate addition and pretreatment," *Journal of Molecular Catalysis A*, vol. 118, no. 1, pp. 89–99, 1997.

[5] Y.-M. Park, D.-W. Lee, D.-K. Kim, J.-S. Lee, and K.-Y. Lee, "The heterogeneous catalyst system for the continuous conversion of free fatty acids in used vegetable oils for the production of biodiesel," *Catalysis Today*, vol. 131, no. 1–4, pp. 238–243, 2008.

[6] A. A. Kiss, A. C. Dimian, and G. Rothenberg, "Solid acid catalysts for biodiesel production—towards sustainable energy," *Advanced Synthesis and Catalysis*, vol. 348, no. 1-2, pp. 75–81, 2006.

[7] S. Furuta, H. Matsuhashi, and K. Arata, "Catalytic action of sulfated tin oxide for etherification and esterification in comparison with sulfated zirconia," *Applied Catalysis A*, vol. 269, no. 1-2, pp. 187–191, 2004.

[8] E. I. Ross-Medgaarden, W. V. Knowles, T. Kim et al., "New insights into the nature of the acidic catalytic active sites present in ZrO_2-supported tungsten oxide catalysts," *Journal of Catalysis*, vol. 256, no. 1, pp. 108–125, 2008.

[9] N. Takahashi, A. Suda, I. Hachisuka, M. Sugiura, H. Sobukawa, and H. Shinjoh, "Sulfur durability of NO_x storage and reduction catalyst with supports of TiO_2, ZrO_2 and ZrO_2-TiO_2 mixed oxides," *Applied Catalysis B*, vol. 72, no. 1-2, pp. 187–195, 2007.

[10] N. Lucas, A. Bordoloi, A. P. Amrute et al., "A comparative study on liquid phase alkylation of 2-methylnaphthalene with long chain olefins using different solid acid catalysts," *Applied Catalysis A*, vol. 352, no. 1-2, pp. 74–80, 2009.

[11] C. Su, J. Li, D. He, Z. Cheng, and Q. Zhu, "Synthesis of isobutene from synthesis gas over nanosize zirconia catalysts," *Applied Catalysis A*, vol. 202, no. 1, pp. 81–89, 2000.

[12] X. M. Liu, G. Q. Lu, and Z. F. Yan, "Nanocrystalline zirconia as catalyst support in methanol synthesis," *Applied Catalysis A*, vol. 279, no. 1-2, pp. 241–245, 2005.

[13] H. Tsuchiya, J. M. MacAk, L. Taveira, and P. Schmuki, "Fabrication and characterization of smooth high aspect ratio zirconia nanotubes," *Chemical Physics Letters*, vol. 410, no. 4–6, pp. 188–191, 2005.

[14] S. Ismail, Z. A. Ahmad, A. Berenov, and Z. Lockman, "Effect of applied voltage and fluoride ion content on the formation of zirconia nanotube arrays by anodic oxidation of zirconium," *Corrosion Science*, vol. 53, no. 4, pp. 1156–1164, 2011.

[15] J. Zhao, X. Wang, R. Xu, F. Meng, L. Guo, and Y. Li, "Fabrication of high aspect ratio zirconia nanotube arrays by anodization of zirconium foils," *Materials Letters*, vol. 62, no. 29, pp. 4428–4430, 2008.

[16] W. J. Lee and W. H. Smyrl, "Oxide nanotube arrays fabricated by anodizing processes for advanced material application," *Current Applied Physics*, vol. 8, no. 6, pp. 818–821, 2008.

[17] L. N. Wang and J. L. Luo, "Enhancing the bioactivity of zirconium with the coating of anodized ZrO_2 nanotubular arrays prepared in phosphate containing electrolyte," *Electrochemistry Communications*, vol. 12, no. 11, pp. 1559–1562, 2010.

[18] L. Guo, J. Zhao, X. Wang, X. Xu, H. Liu, and Y. Li, "Structure and bioactivity of zirconia nanotube arrays fabricated by anodization," *International Journal of Applied Ceramic Technology*, vol. 6, no. 5, pp. 636–641, 2009.

[19] J. R. Sohn and D. H. Seo, "Preparation of new solid superacid catalyst, zirconium sulfate supported on γ-alumina and activity for acid catalysis," *Catalysis Today*, vol. 87, no. 1–4, pp. 219–226, 2003.

Journal of
Nanotechnology

International Journal of
Corrosion

International Journal of
Polymer Science

Smart Materials
Research

Journal of
Composites

BioMed
Research International

Journal of
Materials

Journal of
Metallurgy

Submit your manuscripts at
http://www.hindawi.com

Journal of
Nanoparticles

Advances in
Materials Science and Engineering

Scientifica

Journal of
Nanomaterials

The Scientific
World Journal

International Journal of
Biomaterials

Journal of
Nanoscience

Journal of
Coatings

Journal of
Crystallography

Journal of
Ceramics

Journal of
Textiles